Gas-phase hydrodechlorination of pentachlorophenol over supported nickel catalysts

Eun-Jae Shin and Mark A. Keane [*]

Department of Chemical Engineering, The University of Leeds, Leeds LS2 9JT, UK
E-mail: chemaak@leeds.ac.uk

Received 21 December 1998; accepted 18 February 1999

The gas-phase hydrodechlorination of pentachlorophenol (*PCP*) over nickel/silica and nickel/Y zeolite catalysts at 573 K has been studied. Each catalyst was 100% selective in cleaving the C–Cl bonds, leaving the hydroxyl substituent and benzene ring intact. The variation of catalytic activity and selectivity (in terms of partial and full dechlorination) with time-on-stream is illustrated and catalyst deactivation is addressed. Dechlorination efficiency is quantified in terms of dechlorination rate constants, phenol selectivity/yield and the ultimate partitioning of chlorine in the parent organic and product inorganic host. Increasing the nickel loading on silica was found to raise the overall level of dechlorination while the use of a zeolite support introduced spatial constraints that severely limited the extent of dechlorination. Product composition was largely determined by steric effects where resonance stabilisation had little effect. The reaction pathways, with associated pseudo-first-order rate constants, are also presented.

Keywords: catalytic hydrodechlorination, nickel/silica, nickel/zeolite, pentachlorophenol, dechlorination kinetics

1. Introduction

While chlorinated organics are still important components in commercial processes, they do represent a class of highly toxic and environmentally undesirable compounds, the safe handling of which is now of grave concern [1]. The most widely used disposal method is incineration which does not demonstrate an efficient use of resources and can result in the generation of even more hazardous byproducts [2]. An alternative approach is to detoxify the hazardous waste by chemical processing, whereby the waste is transformed into recyclable raw material and/or product(s). Catalytic hydrogen treatment is now emerging as a low-energy detoxification methodology that converts toxic organic chlorides into the corresponding hydrocarbons (and hydrogen chloride) under moderate conditions [2,3]. Pentachlorophenol (*PCP*) is a persistent organic pollutant extensively used as a wood preservative, pesticide and fungicide, but *PCP* emissions have been severely curtailed by increasingly stricter legislation [4]. While the biodegradation of *PCP* using a range of microorganisms has now been reported [5–7], the authors could find no published study of catalytic hydroprocessing as a means of handling or treating *PCP*. Limited reaction data are, however, available for the catalytic treatment of monochlorophenols [8–11] and dichlorophenols [12,13] in the liquid [8] and gas [9–13] phase. In this study, we describe the gas-phase hydrodechlorination of *PCP* using silica- and zeolite-supported nickel catalysts. We report herein dechlorination rate constants and selectivities, address the nature of the reactant/catalyst interaction(s) and identify reaction pathways involving both stepwise and concerted routes for chlorine removal.

2. Experimental

A 1.5 and a 15.2% w/w Ni/SiO_2 were prepared by homogeneous precipitation/deposition [14] and the catalytic action of each was compared with a 2.2% w/w Ni/Na-Y zeolite prepared by ion exchange [15]. The hydrated samples (sieved in the 150–200 μm mesh range) were reduced *in situ*, without a precalcination step, by heating in a 100 $cm^3\,min^{-1}$ stream of dry hydrogen (99.9%) at a fixed rate of 5 $K\,min^{-1}$ (controlled using a Eurotherm 91e temperature programmer) to a final temperature of 673 ± 1 K which was maintained for 18 h. Catalyst characterisation is described in some detail elsewhere [14–16]. Under these activation conditions, the 1.5% Ni/SiO_2, 15.2% Ni/SiO_2 and 2.2% Ni/Na-Y samples support 1.1×10^{20}, 5.2×10^{20} and 5.4×10^{18} exposed nickel atoms per gram with average nickel particle sizes of 1.4, 3.1 and 39 nm, respectively. All the catalytic reactions were carried out under atmospheric pressure in a fixed-bed glass reactor (i.d. = 15 mm). The catalyst was supported on a glass frit and a layer of glass beads above the catalyst bed ensured that the reactants were vaporised and reached the reaction temperature before contacting the catalyst. The catalytic reactor/procedure has been described previously [17] but some pertinent details are given below. A Merck–Hitachi LC-6000A pump was used to deliver the methanolic solution of *PCP* at a fixed rate, which had been carefully calibrated and the vapour was carried through the catalyst bed in a stream of purified hydrogen. The *PCP* hy-

---

[*] To whom correspondence should be addressed.

drodechlorination activities and selectivities of the three catalyst systems were compared at 573 K and at a fixed W/F value equal to 67 $\mathrm{g\,mol^{-1}\,h}$, where W is the weight of activated catalyst and F is the molar flow rate of *PCP*: the partial pressures of *PCP*, methanol and hydrogen were equal to 0.04, 0.16 and 0.8 atm, respectively. Conversion has been shown previously to be proportional to W/F over the range 17–134 $\mathrm{g\,mol^{-1}\,h}$, which is indicative of an adherence to pseudo-first-order kinetics [13]. The conversion of representative trichlorophenol (2,4,5-*TCP*) and dichlorophenol (2,3-*DCP*) reactants under the same process conditions was also studied for comparative purposes. At the end of each catalytic run the catalyst was regenerated in flowing dry hydrogen at 673 K (for at least 12 h) before reverting to the reaction temperature. The reactor effluent was frozen in a liquid nitrogen trap for subsequent analysis, which was made using an AI Cambridge GC94 chromatograph equipped with a flame ionization detector and employing a DB-1 50×0.20 m i.d., 0.33 μm capillary column (J&W Scientific). Data acquisition and analysis were performed using the JCL 6000 (for Windows) chromatography data system. Fractional conversion is defined as $(m_\mathrm{i} - m_\mathrm{o})/(m_\mathrm{i})$, where m_i is the initial concentration or number of moles of *PCP* entering the reactor per unit time and m_o is the number of moles of *PCP* exiting the reactor per unit time. Molar selectivity (as a percentage) in terms of product n is defined by $m_n/m_\mathrm{tot} \times 100$, where m_tot is the total number of moles of product while the percentage yield is given by $m_n/m_\mathrm{i} \times 100$. The system of linear differential equations that describe the overall *PCP* dechlorination kinetics was solved analytically using a commercial mathematical package (Maple V). A chlorine mass balance was achieved by passing the effluent gas through an aqueous NaOH (3.5–8.0×10^{-3} $\mathrm{mol\,dm^{-3}}$, kept under constant agitation at $\geqslant$300 rpm) trap and monitoring continuously the pH change by means of a Hanna HI programmable printing pH bench-meter [18]; qualitative analysis for the presence of chlorine gas was negative and confirmed that HCl was the only inorganic product. All the reactants were AnalaR grade and were used without further purification.

3. Results and discussion

The results of the catalytic hydrodechlorination of *PCP* using the three nickel catalysts are summarised in table 1 where the lower and higher nickel-loaded silica samples are denoted Ni/SiO$_2$-A and Ni/SiO$_2$-B, respectively. The hydrogen treatment of *PCP* over both silica-based samples generated partially dechlorinated dichlorophenol (2,3-*DCP*, 3,5-*DCP*) and chlorophenol (2-*CP*) as well as the fully dechlorinated phenol as the only products. The catalyst was 100% selective in cleaving the aromatic C-substituent Cl bonds, where the benzene ring and hydroxyl group remained intact. The same catalyst has been shown to effectively hydrogenate phenol to cylohexanone and cyclohexanol while benzene was formed at temperatures in excess of 523 K via hydrogenolysis of the hydroxyl substituent [17]. The isolation of *DCP*s and *CP* in the product stream is indicative of a stepwise removal of chlorine as has been proposed elsewhere [19,20]. The presence of the chlorine substituents shifts the preferred reaction route from hydrogenation/hydrodeoxygenation to hydrodechlorination. The formation of the active surface reactant(s) must involve a direct interaction between the chlorine component and the catalyst resulting in single and multiple dechlorination steps followed by a desorption of the partially or fully dechlorinated phenol. The porous crystalline structure of zeolites can be expected to impose geometrical constraints in terms of product composition and a complete dechlorination of *PCP* to phenol was not observed for the Ni–Na/Y catalyst, where product desorption occurred after the removal of one or two chlorine atoms to form two trichlorophenols (2,3,5-*TCP*/2,4,5-*TCP*) and one dichlorophenol (2,5-*DCP*), respectively.

Table 1

Reaction products, dechlorination rate constants, phenol yields and process selectivities resulting from the hydrogen treatment of *PCP* at 573 K.

Catalytic parameter	Ni/SiO$_2$-A	Ni/SiO$_2$-B	Ni–Na/Y
Products	2,3-*DCP* 3,5-*DCP* 2-*CP*, phenol	2,3-*DCP* 3,5-*DCP* 2-*CP*, phenol	2,3,5-*TCP* 2,4,5-*TCP* 2,5-*DCP*
10^2 $\mathrm{kmol\,h^{-1}\,g_{Ni}^{-1}}$	27.3	5.8	10.9
Y_phenol (%)	4.2	14.0	0
$\mathrm{Cl_{organic}/Cl_{inorganic}}$	4.9	2.6	51.9
Process selectivities (%)			
2,3,5-*TCP*	0	0	8
2,4,5-*TCP*	0	0	66
2,3-*DCP*	40	36	0
2,4-*DCP*	0	0	26
3,5-*DCP*	27	13	0
2-*CP*	16	21	0
phenol	17	30	0

The fractional conversion (x) of *PCP* over the three catalyst systems is illustrated in figure 1 as a function of time-on-stream. In each case there was a decided decline in activity with increasing process time. The loss of hydrodechlorination activity in related systems [21,22] has been attributed to the presence of the HCl that is generated in the reaction which forms stable surface chloride species that block the active sites to the incoming *PCP* reactant. Deactivation is more marked in the case of Ni/Na-Y, where hydrodechlorination activity was negligible after ca. 3 h on-stream. The zeolite-supported system is also susceptible to pore blocking which has been shown elsewhere [23,24] to severely reduce reaction rate. In terms of the reaction kinetics, the reactor was operated in an integral regime and the dechlorination data can be approximated by pseudo-first-order rate expressions where

$$\ln\left(\frac{1}{1-x}\right) = k\left(\frac{W}{F}\right) \tag{1}$$

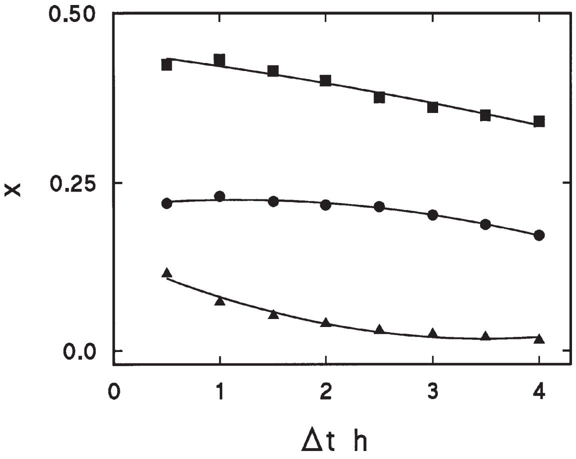

Figure 1. Fractional *PCP* conversion (x) over Ni/SiO$_2$-A (●), Ni/SiO$_2$-B (■) and Ni–Na/Y (▲) as a function of time-on-stream.

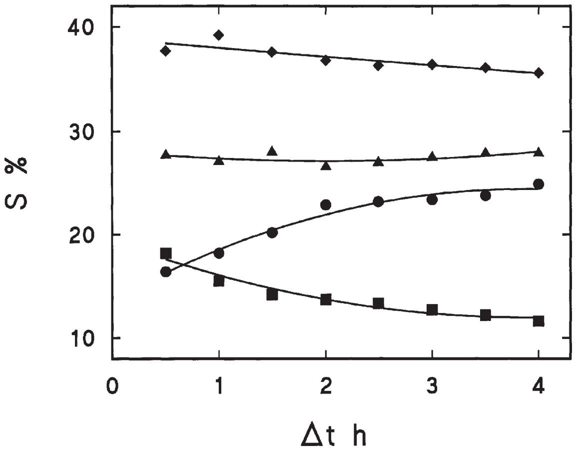

Figure 2. Variation of selectivity with time-on-stream in terms of 3,5-*DCP* (▲), 2,3-*DCP* (◆), 2-*CP* (■) and phenol (●) production resulting from the hydroprocessing of *PCP* over Ni/SiO$_2$-A.

and k represents the overall rate constant. The effective use of the supported nickel metal phase can be assessed by comparing the initial (by extrapolation as described previously [11]) pseudo-first-order rate constants given in table 1. Although the conversion of a fixed feed concentration was higher over Ni/SiO$_2$-B, the lower loaded Ni/SiO$_2$-A delivered the higher k value, indicative of a more effective use of the supported nickel content. The effect of time on process selectivity is illustrated in figure 2, taking Ni/SiO$_2$-A as representative of both silica based systems. The observed continual increase in phenol selectivity is mirrored by the decreasing appearance of 2-*CP* and (to a lesser extent) 2,3-*DCP* in the product stream where 3,5-*DCP* selectivity was largely time invariant. Benzene has been shown to adsorb on nickel systems via the ring π-electron where the ring is parallel to the surface [25]. In the case of *PCP* the principal or catalytically significant interaction(s) is assumed to be through the chlorine component and in such a sterically constrained system the repulsive potential due to the hydroxyl group and neighbouring chlorines will have a considerable bearing on spatial arrangements relative to the surface and the consequent reaction selectivity. Dechlorination has been shown elsewhere [11,18] to proceed via an electrophilic mechanism involving spillover hydrogen and associatively adsorbed chloroaromatic. There is persuasive evidence [26,27] for the co-existence of charged (H^+) and uncharged (H atoms) spillover hydrogen on silica, where the former can be considered to act as the reactive species in catalytic hydrodechlorination. The contribution of a possible resonance effect should be evident from the product composition in that the relative stability of the delocalised carbocation intermediates that result from the electrophilic attack will determine the preferred product. From a consideration of resonance stabilisation effects alone, the most likely partial dechlorination products should be 2,3,5-*TCP*, 2,3-*DCP*, 2,5-*DCP* and 3-*CP*. The product composition (table 1) resulting from catalysis provides no clear match and resonance stabilisation can be taken to have no real influence on product distribution. The generation of 3,5-*DCP* as a principal product is consistent with an approach of *PCP* to the catalyst surface, where the hydroxyl group is pointing away from the surface, the benzene ring is essential parallel to the plane of the surface and in order to relieve the strain, the alternative chlorines bonded to C3 and C5 are directed away from the catalyst. The *PCP* reactant is then fixed to the catalyst through the C2, C4 and C6 chlorines which are attacked concomitantly by hydrogen followed by desorption of the 3,5-*DCP* product. Alternatively, the *PCP* reactant may only interact through one or two of the chlorine substituents, where bond cleavage is followed by a “rollover” of the molecule and immediate additional Cl–catalyst interaction(s)/dechlorination(s) prior to desorption. The generation of 2,3-*DCP* suggests a second possible mode of adsorption involving the chlorines bonded to C4, C5 and C6, where the remaining chlorines and the hydroxyl substituent are oriented away from the catalyst and the benzene ring is canted perpendicular to the plane of the surface. The generation of 2-*CP* and phenol may result from a concerted attack of *PCP* or further dechlorination of the *DCP*(s) that is formed. The isolation of 2-*CP* as the only monochlorinated product is indicative of appreciable positional considerations where the chlorine that is positioned *ortho* to –OH is less susceptible to attack by hydrogen. With increasing process time, complete dechlorination to phenol was preferentially promoted, as is more clearly revealed in figure 3. This is in marked contrast to the hydrogen treatment of 2,4,5-*TCP*, as a representative trichlorophenol, where phenol selectivity decreased markedly as the overall conversion (shown in the inset to figure 3) declined. In contrast, the conversion of 2,3-*DCP*, as a representative dichlorophenol, and the resultant phenol selectivity were both essentially independent of process time.

In the hydroprocessing of *PCP* over Ni–Na/Y, 2,3,5-*TCP* was formed with increasing selectivity at the direct loss of selectivity in terms of 2,4,5-*TCP* and 2,4-*DCP* production. Indeed, there is a linear relationship, shown in figure 4, between product selectivity and the loss of catalytic activity, expressed as the ratio of time-dependent (x_t) to

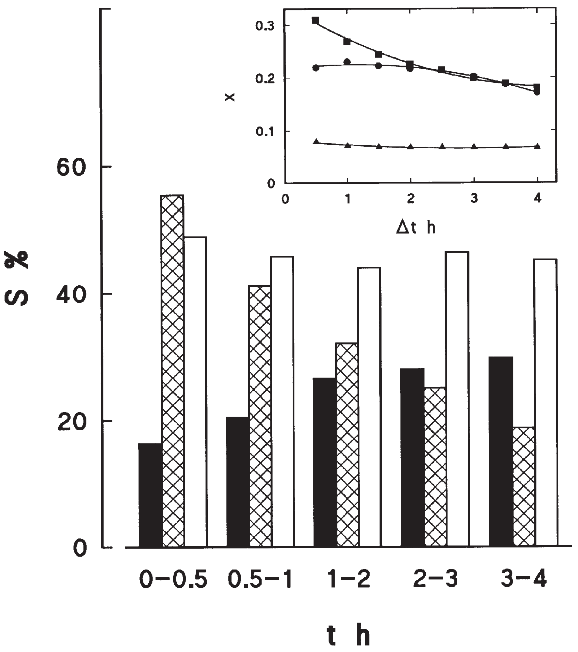

Figure 3. Effect of process time on phenol selectivity resulting from the hydrogen treatment of *PCP* (solid bars), 2,4,5-*TCP* (cross-hatched bars) and 2,3-*DCP* (open bars) over Ni/SiO$_2$-A. Inset: time dependence of the fractional conversion of *PCP* (●), 2,4,5-*TCP* (■) and 2,3-*DCP* (▲).

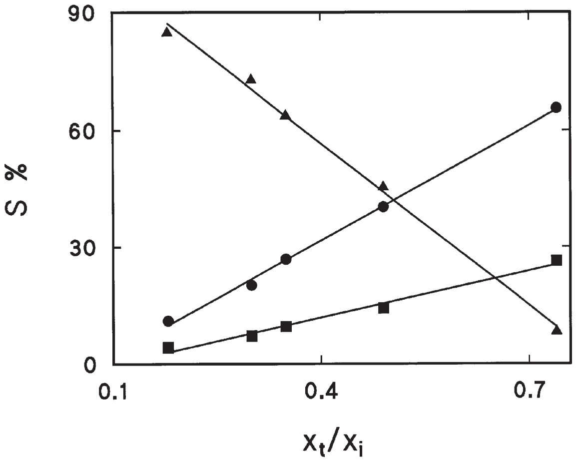

Figure 4. Process selectivity in terms of 2,3,5-*TCP* (▲), 2,4,5-*TCP* (●) and 2,4-*DCP* (■) formation over Ni–Na/Y as a function of time-dependent (x_t) to initial (x_i) fractional conversion.

initial (x_i) fractional conversion. The product 2,4,5-*TCP* can be viewed as an intermediate in the formation of 2,4-*DCP* where the concomitant loss of selectivity supports a common reaction pathway. The preferential formation of 2,3,5-*TCP* can be taken to coincide with increasing pore blockage where the preferred common removal of chlorines that are separated by two- rather than three-ring C–C bonds may be attributed to a crowding effect. In terms of dechlorination efficiency, the higher loaded Ni/SiO$_2$-B sample was more selective in terms of phenol formation, delivered higher phenol yields and there was a decided shift in favour of more complete dechlorination when compared with Ni/SiO$_2$-A. As Ni/SiO$_2$-B supports larger nickel metal particles, such observations suggest the possible involvement of an ensemble effect. The zeolite system is characterised by even larger metal crystallites but there is an appreciable smaller particle component accommodated within the zeolite pore structure which serves to promote hydrodechlorination. The ultimate dechlorination efficiency may, however, be determined by such considerations as acidity, porosity and coking. The explicit assignment of a surface active site is beyond the scope of this report. Work is now underway to characterise the fresh and used catalysts (by TEM, H$_2$ TPD and XPS) in order to relate dechlorination activity/selectivity to catalyst structure. As the replacement of each chlorine by a hydrogen represents a decrease in the toxicity of the parent *PCP*, the overall process can be termed a detoxification. Detoxification efficiency is quantified in table 1 in terms of the ultimate partitioning of chlorine in the parent organic or product inorganic host, i.e., the $Cl_{organic}/Cl_{inorganic}$ ratio. Under the same process conditions, the effluent stream emerging from the Ni–Na/Y catalyst bed retained 1.4 times the amount of chlorine associated with the organic host than that exiting the reactor that contained Ni/SiO$_2$-B which represents an appreciable difference in detoxification levels.

The hydrodechlorination of *PCP* to phenol can follow a stepwise or concerted route. We have shown elsewhere [11] that, under the stated reaction conditions, dechlorination is irreversible and the catalytic conversions are far removed from equilibrium values. In the conversion of *PCP* over Ni/SiO$_2$-A (as a model catalyst), 2,3-*DCP*, 3,5-*DCP* and 2-*CP* represent stable partially dechlorinated intermediates in the generation of phenol according to the following sequence of steps:

$$PCP + 3H_2 \xrightarrow{k_1} 3{,}5\text{-}DCP + 3HCl \tag{2}$$

$$PCP + 3H_2 \xrightarrow{k_2} 2{,}3\text{-}DCP + 3HCl \tag{3}$$

$$PCP + 4H_2 \xrightarrow{k_3} 2\text{-}CP + 4HCl \tag{4}$$

$$PCP + 5H_2 \xrightarrow{k_4} \text{phenol} + 5HCl \tag{5}$$

$$2{,}3\text{-}DCP + H_2 \xrightarrow{k_5} 2\text{-}CP + HCl \tag{6}$$

$$3{,}5\text{-}DCP + 2H_2 \xrightarrow{k_6} \text{phenol} + 2HCl \tag{7}$$

$$2{,}3\text{-}DCP + 2H_2 \xrightarrow{k_7} \text{phenol} + 2HCl \tag{8}$$

$$2\text{-}CP + H_2 \xrightarrow{k_8} \text{phenol} + HCl \tag{9}$$

The rate of consumption of *PCP* and the formation of each partially dechlorinated aromatic and fully dechlorinated phenol can be written as

$$-\frac{d[PCP]}{dW/F} = (k_1 + k_2 + k_3 + k_4)[PCP], \tag{10}$$

$$\frac{d[3{,}5\text{-}DCP]}{dW/F} = k_1[PCP] - k_6[3{,}5\text{-}DCP], \tag{11}$$

$$\frac{d[2{,}3\text{-}DCP]}{dW/F} = k_2[PCP] - (k_5 + k_7)[2{,}3\text{-}DCP], \tag{12}$$

$$\frac{d[2\text{-}CP]}{dW/F} = k_3[PCP] + k_5[2{,}3\text{-}DCP] - k_8[2\text{-}CP], \tag{13}$$

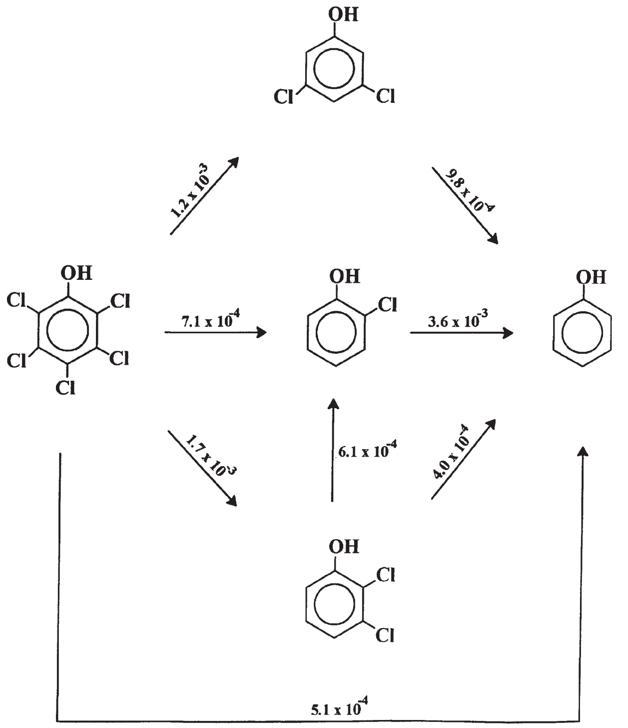

Figure 5. Reaction pathways with the associated pseudo-first-order kinetic rate constants (units = $\mathrm{mol\,h^{-1}\,g^{-1}}$) for the hydrodechlorination of *PCP* over Ni/SiO_2-A.

$$\frac{\mathrm{d[phenol]}}{\mathrm{d}W/F} = k_4[PCP] + k_6[3{,}5\text{-}DCP] + k_7[2{,}3\text{-}DCP] + k_8[2\text{-}CP], \qquad (14)$$

where [ ] denotes concentration and k_1–k_8 are the pseudo-first-order reaction rate constants for each step. The values of k_5–k_8 have been determined in earlier studies [11,13] while k_1–k_4 were calculated using equations (10)–(14) and the experimental activity/selectivity data. The reaction pathways for the conversion of *PCP* are illustrated in figure 5 wherein the pseudo-first-order rate constants associated with each individual dechlorination step are identified. The reaction scheme involves a full dechlorination to phenol via both concerted and stepwise mechanisms. The rate constant ratio for stepwise to concerted attack equals 7.1, which indicates that the stepwise pathway is the predominant one in the generation of phenol from *PCP*.

4. Conclusions

In the gas-phase hydrodechlorination of *PCP* promoted by supported nickel catalysts, the data presented in this paper support the following conclusions:

(i) both silica- and zeolite-based systems are 100% selective in cleaving the C–Cl bonds, leaving the aromatic ring and hydroxyl substituent intact;

(ii) phenol formation occurs via simultaneous and consecutive irreversible steps where the stepwise route predominates;

(iii) steric effects in the adsorption step govern to a greater degree the ultimate product composition where resonance stabilisation has little effect;

(iv) the nickel–silica catalysts are subject to deactivation due to HCl poisoning while Ni–Na/Y exhibits a more acute loss of activity due to the additional contribution of pore blocking;

(v) an increase in nickel loading in the silica system gives rise to an appreciable increase in dechlorination efficiency.

Acknowledgement

EJS acknowledges partial financial support from the British Council.

References

[1] F. Murena, V. Famiglietti and F. Gioia, Environ. Prog. 12 (1993) 233.
[2] A. Converti, M. Zilli, D.M. De Faveri and G. Ferraiolo, J. Hazard. Mater. 27 (1991) 127.
[3] S. Kovenklioglu, Z. Cao, D. Shah, R.J. Farrauto and E.N. Balko, AIChE J. 38 (1992) 1003.
[4] A.J. Buonicore and W. Davis, eds., *Air Pollution Engineering Manual,* Air and Waste Management Association (Van Nostrand Reinhold, New York, 1992).
[5] S. Pallerla and R.P. Chambers, Catal. Today 40 (1998) 103.
[6] G.J. Mileski, J.A. Bumpus, M.A. Jurek and S.D. Aust, Appl. Environ. Microbiol. 54 (1988) 2885.
[7] B.E. Logan, B.C. Alleman and L.A. Gary, Water Res. 28 (1994) 1533.
[8] J.B. Hoke, G.A. Gramiccioni and E.N. Balko, Appl. Catal. B 1 (1992) 285.
[9] S. Chon and D.T. Allen, AIChE J. 37 (1991) 1730.
[10] A.R. Suzdorf, S.V. Morozov, N.N. Anshits, S.I. Tsiganova and A.G. Anshits, Catal. Lett. 29 (1994) 49.
[11] E.J. Shin and M.A. Keane, Appl. Catal. B 18 (1998) 241.
[12] A.R. Suzdorf, S.I. Tsiganova, N.N. Anshits, S.V. Morozov and A.G. Anshits, Sib. Khim. Z. (1992) 131.
[13] E.J. Shin and M.A. Keane, Chem. Eng. Sci., in press.
[14] M.A. Keane, Canad. J. Chem. 72 (1994) 372.
[15] B. Coughlan and M.A. Keane, J. Catal. 123 (1990) 364.
[16] B. Coughlan and M.A. Keane, Zeolites 11 (1991) 2.
[17] E.J. Shin and M.A. Keane, J. Catal. 173 (1998) 450.
[18] G. Tavoularis and M.A. Keane, J. Mol. Catal., in press.
[19] J. Frimmel and M. Zdražil, J. Catal. 167 (1997) 286.
[20] B.F. Hagh and D.T. Allen, AIChE J. 36 (1990) 773.
[21] B. Coq, G. Ferrat and F. Figueras, J. Catal. 101 (1986) 434.
[22] J. Estelle, J. Ruz, Y. Cesteros, R. Fernandez, P. Salagre, F. Medina and J.E. Sueiras, J. Chem. Soc. Faraday Trans. 92 (1996) 2811.
[23] B. Coughlan and M.A. Keane, J. Mol. Catal. 71 (1992) 93.
[24] E.J. Creyghton, M.H.W. Burgers, J.C. Jansen and H. van Bekkum, Appl. Catal. A 28 (1995) 275.
[25] B. Coughlan and M.A. Keane, J. Chem. Soc. Faraday Trans. 86 (1990) 3961.
[26] F. Rossner and U. Roland, J. Mol. Catal. A 112 (1996) 401.
[27] U. Roland, Th. Braunschweig and F. Rossner, J. Mol. Catal. A 127 (1997) 61.